

Factor H-related protein 1 (FHR-1) binds to C-reactive protein and enhances rather than inhibits complement activation

Ádám I. Csicsi,* Zsóka Szabó,* Zsófia Bánlaki,* Barbara Uzonyi,† Marcell Cserhalmi,* Éva Kárpáti,* Agustín Tortajada,‡ Joseph J.E. Caesar,§ Zoltán Prohászka,¶ T. Sakari Jokiranta,|| Susan M. Lea,§ Santiago Rodríguez de Córdoba,‡ Mihály Józsi*

* MTA-ELTE “Lendület” Complement Research Group, Department of Immunology, Eötvös Loránd University, 1117 Budapest, Hungary;

† MTA-ELTE Immunology Research Group, Department of Immunology, Eötvös Loránd University, 1117 Budapest, Hungary;

‡ Department of Cellular and Molecular Medicine, Centro de Investigaciones Biológicas and Ciber de Enfermedades Raras, Madrid, Spain;

§ Sir William Dunn School of Pathology, University of Oxford, Oxford, United Kingdom;

¶ Research Laboratory, 3rd Department of Internal Medicine, Semmelweis University, Budapest, Hungary;

|| Research Programs Unit, Immunobiology, Haartman Institute, University of Helsinki, Finland

Corresponding author: Mihály Józsi, MTA-ELTE “Lendület” Complement Research Group, Department of Immunology, Eötvös Loránd University, Pázmány Péter sétány 1/c, H-1117 Budapest, Hungary; Phone: +36 1 3812175; Fax: +36 1 3812176; E-mail: mihaly.jozsi@gmx.net.

Running title: FHR-1 binds to CRP and modulates complement activation

Abstract

Factor H (FH)-related protein 1 (FHR-1) is one of the five human factor H-related proteins, which share sequence and structural homology with the alternative pathway complement inhibitor FH. Genetic studies on disease associations and functional analyses indicate that FHR-1 enhances complement activation by competitive inhibition of FH binding to some surfaces and immune proteins. We have recently shown that FHR-1 binds to pentraxin 3. Here, our aim was to investigate whether FHR-1 binds to another pentraxin, C-reactive protein (CRP), analyze the functional relevance of this interaction and study the role of FHR-1 in complement activation and regulation. FHR-1 did not bind to native, pentameric CRP but it bound strongly to monomeric CRP via its C-terminal domains. FHR-1 at high concentration competed with FH for CRP binding, indicating possible complement de-regulation also on this ligand. FHR-1 did not inhibit regulation of solid phase C3 convertase by FH and did not inhibit terminal complement complex formation induced by zymosan. On the contrary, by binding C3b, FHR-1 allowed C3 convertase formation and thereby enhanced complement activation. FHR-1/CRP interactions increased complement activation via the classical and alternative pathways on surfaces such as the extracellular matrix and necrotic cells. Altogether, these results identify CRP as a ligand for FHR-1 and suggest that FHR-1 enhances rather than inhibits complement activation, which may explain the protective effect of FHR-1 deficiency in age-related macular degeneration.

Keywords: alternative complement pathway, classical complement pathway, C-reactive protein, complement activation, complement deregulation, pentraxin, FHR-1

Introduction

The human factor H protein family includes the major alternative pathway regulator factor H (FH), its splice variant factor H-like protein 1 (FHL-1), and five factor H-related proteins (FHRs) (1). All members of this protein family are composed exclusively of complement control protein (CCP) domains (also known as short consensus repeats, SCRs). While the function of FH is well characterized, the role of the FH-related proteins is incompletely understood (1, 2).

Despite the limited information on FHR protein functions, genetic studies linked the FHR proteins to various diseases (reviewed in (1)). The five *CFHR* genes have arisen through segmental duplications (3, 4), and this makes the genomic region encoding the FH and the five FHRs prone to misalignments and genomic recombination events. These may result in hybrid proteins involving FH and FHR-1 or FHR-3, gene conversion events, e.g. between the exons coding for the C termini of FH and FHR-1, gene deletions affecting *CFHR1*, *CFHR3* and *CFHR4*, as well as in duplication of exons (reviewed in (1)). The *CFH::CFHR1* and *CFHR1::CFH* hybrid genes are associated with atypical hemolytic uremic syndrome (aHUS) (5-7), the deletion of the *CFHR1* gene predisposes to the autoimmune form of aHUS (8, 9), and a mutant FHR-1 protein with duplicated CCPs 1-2 was described as pathogenic in a patient with C3 glomerulopathy (10). These data indicate a role of FHR-1 in the regulation or modulation of complement activation.

FHR-1 is the most abundant glycoprotein among the FHRs, with estimated plasma concentration of 40-100 µg/ml (11, 12). It is composed of five CCPs that are homologous to CCPs 6-7 and CCPs 18-20 of FH (13). Two FHR-1 glycoforms, FHR-1α (37 kDa) and FHR-1β (43 kDa) are detected in plasma, representing differentially glycosylated proteins (11). In addition, an acidic (FHR-1*A) and a basic (FHR-1*B) isoform of the protein exist, that differ in sequence in three amino acids (14). The CCPs 3, 4 and 5 of FHR-1 have a high degree of amino acid sequence identity (95%, 100% and 97% in FHR-1*A and 100%, 100% and 97% in FHR-1*B, respectively) to the three most C-terminal domains of FH (**Fig. 1**). These FH domains are responsible for host surface recognition and contain an important C3b-binding site (15-19).

The homology between FHR-1 and FH suggests related functions and, indeed, FHR-1 binds to C3b (12, 20), although FH, having three binding sites for C3b, shows more pronounced binding. No cofactor activity and convertase decay accelerating activity were observed for FHR-1 at the C3b and C3 convertase level in line with the lack of homologous domains in FHR-1 to the complement regulatory domains of FH (11, 12). FHR-1 was described as an inhibitor of C5 convertase and formation of the terminal pathway membrane attack complex (12), but other groups could not confirm this activity (20, 21). CCP1 and CCP2 of FHR-1 display only weak similarity to the respective CCPs of FH (42% and 34% amino acid identity to CCP6 and CCP7 of FH, respectively), but are almost identical to CCPs 1-2 of FHR-2 and FHR-5. These domains contain a unique dimerization motif that allows for FHR-1, FHR-2 and FHR-5 to exist as dimeric species *in vivo*. Moreover, dimerization is thought to increase avidity for ligands and enhance the ability of FHR-1, FHR-2 and FHR-5 to compete with FH for C3b binding *in vitro* (21).

The FH C terminus contains binding site, in addition to C3b, for heparin and mediates cell surface binding such as attachment to endothelial cells, which was also described for FHR-1 (12, 20). Moreover, these FH domains contain binding sites for the pentraxins pentraxin 3 (PTX3) and C-reactive protein (CRP) (22-24). FHR-1 binding to PTX3 was described (23) but its interaction with CRP has not yet been analyzed.

CRP is a 115-kDa acute-phase protein with a disc-like form composed of five identical subunits, which are assembled non-covalently (25). The structure is stabilized by Ca^{2+} in human plasma, but CRP dissociates into its monomeric subunits in the absence of calcium, at low pH or at increased temperature (25-27). CRP levels in the plasma of healthy adults are low, with a median concentration of 0.8 $\mu\text{g/ml}$, but they increase as much as a 1000-fold during acute phase reaction (28). Several ligands have been identified for CRP, including microorganisms, phosphorylcholine, complement components (e.g., C1q, FH, C4b-binding protein, ficolins), and proteins of the extracellular matrix, but the relationship between ligand binding and function is a matter of debate in most cases (25, 29). Surface-bound CRP has been shown to inhibit the alternative pathway, possibly through the interaction with FH (30, 31). The FH and FHL-1 402H variants, which are strongly associated with increased risk to develop age-related macular degeneration (AMD), were shown to bind CRP less strongly compared with the 402Y variants (32, 33). This interaction – among others – is thought to be important in the pathogenesis of AMD. The common *CFHR3-CFHR1* gene deletion, causing FHR-1 deficiency, is protective in AMD (34).

Therefore, the aim of this study was to evaluate FHR-1 as a potential ligand for CRP and analyze the functional relevance of this interaction. We also aimed to investigate whether FHR-1, similar to FHR-4 and FHR-5 (35, 36), has a role in complement activation by supporting formation of the C3bBb convertase.

Materials and Methods

Proteins, antibodies and sera

Recombinant human FHR-1*A (referred to as FHR-1 in the paper), FHL-1, FHR-4A and FHR-4B were generated using the pBSV-8His Baculovirus expression vector (37), expressed in *Spodoptera frugiperda* (Sf9) cells, and purified by nickel-affinity chromatography as described (23, 38, 39). Recombinant human FHR-5, PTX3, and biotinylated goat anti-human PTX3 antibody were obtained from R&D Systems (Wiesbaden, Germany). Recombinant human FHR-2-gst fusion protein was purchased from Abnova (Taipei, Taiwan) and FHR-3-gst fusion protein was purchased from Proteintech Europe (Manchester, UK). The C-terminal fragments of FH and the FHR proteins were generated as described (21). FHR-1*A and FHR-1*B were isolated from human plasma as described (23). Recombinant FH19-20 fragment with 14 different single amino acid substitutions were produced in yeast cells (40).

Purified human FH, C3, C3b, factor B (FB), factor D (FD), properdin (factor P; FP) factor I (FI), C1q, C1, recombinant human CRP, goat anti-human FH antibody, goat anti-human FB antibody, goat anti-human C1q antibody and goat anti-human C4 antibody were obtained from Merck Ltd. (Budapest, Hungary). mCRP was generated from recombinant CRP by urea/EDTA chelation treatment as described previously (24). The anti-FH mAbs A254 and A255, and the anti-FP mAb A235 were from Quidel (Biomedica, Budapest, Hungary). The anti-FH mAb C18 (41) was purchased from Alexis Biochemicals (Lörrach, Germany). The goat anti-CRP antibody and the anti-mCRP mAb (clone CRP-8) were from Sigma-Aldrich Ltd. (Budapest, Hungary). The anti-pCRP mAb was purchased from Antibodies-online GmbH (Aachen, Germany). Horseradish peroxidase (HRP)-conjugated goat anti-human C3 was from MP Biomedicals (Solon, OH). HRP-conjugated swine anti-rabbit immunoglobulins, rabbit anti-goat immunoglobulins and goat anti-mouse immunoglobulins were from Dako (Hamburg, Germany).

Normal human plasma was collected from healthy individuals and pooled, and sera from patients with sepsis or aHUS were obtained according to protocols approved by the institutional review board of Semmelweis University of Budapest and the National Ethical Committee (Scientific and Research Ethics Committee of the Medical Research Council).

Written approvals for the diagnostic tests and research analysis were given by the patients or their parents. IgG fractions of aHUS patients with FH autoantibodies and of healthy individuals were isolated from serum or plasma using Protein G columns as described (23). FH-depleted human serum was purchased from Complement Technology (Tyler, Texas, US).

Western blot

To analyze binding of native FHR-1 from human plasma to CRP, microplate wells were coated with 10 µg/ml CRP or gelatin in DPBS (Lonza, Cologne, Germany). Wells were incubated with 50% v/v NHS in DPBS (with Ca^{2+} and Mg^{2+}) for 1 h at 37°C. After washing, the bound proteins were eluted with non-reducing SDS-sample buffer, separated on 10% SDS-PAGE and transferred to nitrocellulose membrane. The blot was incubated with a polyclonal goat anti-FH antibody and the corresponding secondary antibody, and developed with an ECL detection kit (Merck).

Microtiter plate binding assays

To measure binding of CRP to FHRs at various pH, 5 µg/ml FH, FHR-1, FHR-5 and HSA were immobilized in microtiter plate wells and, after blocking with 4% BSA (w/v) in DPBS, 2.5% v/v NHS or sepsis serum, or 5 µg/ml recombinant CRP, were added in DPBS (with Ca^{2+} and Mg^{2+}) at pH values 7.4, 6.5 and 5.5. CRP was detected with the goat anti-human CRP antibody that recognizes both CRP forms (42) and HRP-conjugated rabbit anti-goat immunoglobulin. TMB PLUS substrate (Kem-En-Tec Diagnostics, Taastrup, Denmark) was used to visualize binding and the absorbance was measured at 450 nm.

Interaction of FHRs with pCRP was measured in TBS (10 mM Tris, 140 mM NaCl, 2 mM CaCl_2 , 1 mM MgCl_2 [pH 7.4]). FH, FHR proteins and human serum albumin (HSA) as control protein were immobilized at 65 nM in microplate wells and, after blocking with 3% BSA (w/v) in TBS, incubated with up to 50 µg/ml pCRP. CRP binding was detected with the goat anti-human CRP antibody.

To measure mCRP binding to FHR proteins, FHR proteins and their C-terminal fragments were immobilized in microtiter plate wells at 5 µg/ml concentration, followed by blocking with 3% BSA (w/v) in DPBS and incubation with 10 µg/ml mCRP. Binding of mCRP was detected as described above.

In some assays, 5 µg/ml CRP was immobilized in microplate wells in DPBS, which results in the decay of most bound CRP into the mCRP form (42). After blocking, FHR-1, FHR-5 and FH were added in serial dilutions for 1 h at 20°C and their binding was detected using the goat anti-FH antibody.

To compare binding of mCRP to FHR-1*A and FHR-1*B, the two FHR-1 variants were immobilized at 4 µg/ml in DPBS in microplate wells, and binding of increasing amounts of mCRP was measured as described above.

To analyze PTX3 binding by FH19-20 mutants, microtiter plates were coated with 4 µg/ml each of the wild-type or mutant FH19-20 fragments, diluted in TBS in 25 µl, overnight at 4°C. The wells were washed after each step with TBS containing 0.05% Tween-20 (v/v). After blocking with 4% BSA (w/v) in TBS for 1 h at 20°C, 5 µg/ml PTX3 was added in TBS for 1 h at 37°C. Bound PTX3 was detected with a biotinylated goat anti-PTX3 antibody followed by HRP-conjugated streptavidin.

To measure C1q binding to FHR-1-bound mCRP, microplate wells were coated with 4 µg/ml recombinant FHR-1 and, as control, with gelatin, and then incubated with 5 µg/ml mCRP for 1 h at 20°C. After washing with DPBS containing 0.05% Tween-20 (v/v), C1q was added in increasing concentrations for 1 h at 20°C, and C1q binding was detected using anti-C1q and the corresponding secondary antibody. Binding of C1 was similarly measured by incubating the wells with 10 µg/ml C1 instead of C1q.

In inhibition assays, 5 µg/ml FHR-1 was immobilized in microplate wells. The mAbs C18 and A255 were added in 10 µg/ml in DPBS, and IgG fractions derived from sera of aHUS patients containing FH autoantibodies or sera of healthy individuals, were added in 500 µg/ml, for 15 min at 20°C, followed by the addition of mCRP in 5 µg/ml final concentration. The binding of mCRP was detected as described above.

Competition assays

To measure competition between PTX3 and mCRP, immobilized FHR-1 (5 µg/ml) was incubated with 5 µg/ml PTX3 in the absence or presence of serial dilutions of mCRP in microtiter plate wells. Bound PTX3 was detected with a biotinylated goat anti-human PTX3 antibody.

For FH 15-20/FHR-1 inhibition assays, 10 µg/ml recombinant FH 15-20 fragment was immobilized and incubated with 5 µg/ml mCRP in the absence or presence of 1 µM FHR-1. Bound mCRP was measured with a polyclonal goat anti-human CRP antibody and the corresponding secondary antibody. Competition of FHR-1 with FHL-1 was similarly measured.

C3 convertase assembly and decay accelerating activity assays

To measure the effect of FHR-1 on the assembly and activity of the C3bBb alternative pathway C3 convertase, C3b was immobilized at 5 µg/ml in microplate wells. FH (10 µg/ml), FHR-1 (50 µg/ml), FHR-5 (10 µg/ml), or BSA (50 µg/ml) were added together with FB, FD and properdin to generate C3bBb convertase as described (36). The formed C3bBb was detected using polyclonal anti-FB antibody. The convertase activity was measured by adding 10 µg/ml purified C3 for 1 h at 37°C and quantifying the generated C3a by a C3a ELISA kit (Quidel). Formation of the C3bBb alternative pathway C3 convertase on surface-bound FHR-1 was measured as described previously (36).

To investigate decay accelerating activity of FHR-1, the C3bBb convertase was built up as described (36), then FH (2.5 µg/ml), FHR-1 (10 µg/ml), FHR-5 (10 µg/ml), or FH plus FHR-1 or FH plus FHR-5 were added for 30 minutes at 20°C in DPBS. The remaining convertase was detected with a polyclonal anti-FB antibody.

Cell-derived ECM was prepared by culturing the human retinal pigmented epithelial cell line ARPE-19 (ATCC, LGC Standards GmbH, Wesel, Germany) in 96-well tissue culture plates, coated with 0.2% (w/v) gelatin, in DMEM:F12 medium (Lonza) supplemented with 10% FCS, penicillin (100 U/ml), streptomycin (100 µg/ml), and Amphotericin B (250 ng/ml), in a cell incubator with 5% CO₂ (v/v) at 37°C. Cells were removed by incubation with DPBS containing 20 mM EDTA; removal was controlled visually by microscopy. To measure the formation of the C3bBb C3 convertase on cell-free ECM, the washed ECM was blocked with 4% (w/v) BSA in DPBS containing 0.05% Tween-20 (v/v), then the wells were sequentially incubated with 5 µg/ml mCRP, 50 µg/ml FHR-1, and 50 µg/ml C3b (all in DPBS, 1 hr at 20°C, with washing steps). Purified FB (2 µg/ml), FD (0.2 µg/ml) and FP (4 µg/ml) were added in convertase buffer (containing 2 mM Ni²⁺, 4% (w/v) BSA and 0.05% (v/v) Tween-20) at 37°C for 30 min to generate the C3bBb convertase as described (36). The formed C3bBb was detected with anti-FB antibody as above.

Terminal pathway inhibition assays

To assess possible inhibition of the terminal pathway by FHR-1, complement activation was induced by adding 20 µg/ml zymosan to 30% NHS (v/v) in DPBS in the absence or presence of 1 µM FH, FHR-1 or FH plus FHR-1 in a final volume of 20 µl. After incubation for 30 minutes at 37°C, terminal pathway activation was detected by measuring the generated C5b-9 complexes with a C5b-9 ELISA kit (Quidel).

Complement activation assays

To assess functional consequence of FHR-1/FH competition, 10 µg/ml CRP was immobilized in microtiter plate wells and, after blocking and washing, 20% (v/v) NHS or factor H-depleted serum was added in the absence or presence of 1 µM FHR-1 or 300 nM FHR-5, used as a control protein. After incubation for 30 minutes at 37°C, C3 deposition was detected with a HRP-labeled polyclonal anti-C3 antibody.

To measure complement activation and C3 convertase formation on FHR-1, microtiter plate wells were coated with 5 µg/ml FHR-1, FHR-4B and HSA. After blocking with 4% BSA (w/v) in DPBS, wells were incubated with 10% normal human serum with or without 5 mM Mg²⁺-EGTA or 5 mM EDTA for 30 min at 37°C. Deposition of C3b, FB and FP was detected using the corresponding primary and secondary antibodies as described (35).

To measure classical pathway activation, microplate wells were coated with 4 µg/ml recombinant FHR-1 and, as control, with gelatin, and then incubated with 5 µg/ml mCRP for 1 h at 20°C. After washing with DPBS containing 0.05% Tween-20 (v/v), 1% (v/v) normal human serum in DPBS containing Mg²⁺ and Ca²⁺ (Lonza), or in DPBS containing 20 mM EDTA, was added for 30 min at 37°C. C4-fragment deposition was detected using polyclonal anti-C4 antibody. To measure C4 deposition on ARPE-19 cell-derived ECM, the washed cell-free ECM was sequentially incubated with 20 µg/ml recombinant FHR-1 and 5 µg/ml mCRP, then exposed to 1% human serum. C4 fragments were detected as above.

Flow cytometry

HUVEC were cultured in EGM-2 medium (both from Lonza) supplemented according to the manufacturer's instructions. Confluent cell layer was removed by incubation with Trypsin-EDTA solution (Lonza). Necrosis of HUVEC was induced by heat treatment (65°C, 30 min). Necrotic HUVEC (5 × 10⁵ cells/sample) were left untreated or were preincubated with 2.5 µg/ml mCRP, then incubated with 25 µg/ml recombinant FHR-1 in DPBS containing Mg²⁺ and Ca²⁺ (Lonza). After washing, cells were exposed to 5% normal human serum in buffer containing 5 mM Mg²⁺-EGTA. The C3bBb convertase was detected by serial incubation with anti-FB and Alexa488-labeled rabbit anti-goat Ig antibody (Invitrogen; Thermo Fisher Scientific, Waltham, MA USA). Necrotic cells were gated based on positive staining for propidium iodide. Cells were measured using a DB FACSCalibur flow cytometer (BD Biosciences, Heidelberg, Germany) and CellQuest Pro software, and data were analyzed using FCS Express 3.0 (BD Biosciences).

Visualization of ligand binding sites on FH19-20

Ligand binding sites on FH19-20 (Protein Data Bank accession code 2G7I) (43) were visualized using PyMOL (www.pymol.org).

Statistical analysis

Statistical analysis was performed using GraphPad Prism version 4.00 for Windows (GraphPad Software, San Diego California USA). A *p* value < 0.05 was considered statistically significant.

Results

Binding of the two CRP forms to the FHR proteins

First, we investigated if binding of native FHR-1 to CRP can be detected from human serum. CRP was immobilized in microplate wells, which were then incubated with serum. The bound proteins were eluted and analyzed by SDS-PAGE and Western blotting using polyclonal anti-FH, which detects both FH and FHR-1. This experiment revealed prominent binding of FH

and both FHR-1 glycoforms to CRP (**Fig. 2A**). This assay, however, does not exclude indirect binding, *e.g.* via C3-fragments, which may explain the background binding of FH to the gelatin-coated control well.

The interaction of FHR-1 with CRP was also studied by ELISA. Previously, CRP was shown to bind to several of its ligands in a pH-dependent manner, showing increased binding at slightly acidic pH, which may be observed at inflammatory sites (44). We used serum from a sepsis patient to analyze the binding of native CRP to immobilized FHR-1 at various pH. No CRP binding was detected at pH 7.4, whereas significant binding of CRP to FHR-1 was detected at pH 6.5 and pH 5.5. Similar binding was observed in the case of the FHR-5 protein, whereas no CRP binding to FH was observed under these conditions (**Fig. 2B**). To analyze direct protein interactions, these experiments were also performed using recombinant native pCRP and yielded similar results (**Fig. 2C**).

We set out to clarify which form of CRP interacts with FHR-1. Binding of the native pentameric pCRP to all human FHR proteins was measured by ELISA in Ca^{2+} -containing buffer at physiological pH. To this end, FH family proteins were immobilized in microtiter plate wells and binding of pCRP added in increasing concentrations up to 50 $\mu\text{g/ml}$ (~435 nM) was measured using polyclonal CRP-specific antibody. pCRP bound strongly to FHR-4, as expected (42), and much more weakly to FHR-3 (**Fig. 3A**). There was marginal binding to FHR-5 at the highest investigated pCRP concentration, whereas no pCRP binding to FH, FHR-1 and FHR-2 was observed at this pH. However, mCRP that was generated from pCRP by urea-chelation treatment, showed strong binding to FHR-1, FH and FHR-5 (**Fig. 3B**).

Previously, a mCRP binding site in CCPs 19-20 of FH was identified (24). Therefore, we studied whether the homologous CCPs 4-5 of FHR-1 also harbour a binding site for mCRP. To this end, the homologous C-terminal two domains of all five FHR proteins were studied for mCRP binding in ELISA. CCPs 4-5 of FHR-1 bound mCRP similar to CCPs 19-20 of FH. None of the other homologous FHR C-terminal domains bound mCRP (**Fig. 3B**).

The two FHR-1 allelic variants were also analyzed for mCRP binding using FHR-1*A and FHR-1*B purified from plasma of homozygous carriers of each allele. The two variants bound mCRP equally well (**Fig. 3C**).

Binding of FHR-1 to surface-bound CRP was measured by ELISA. To this end, CRP was immobilized in microplate wells, resulting in the generation of mCRP (42), and serial dilutions of FHR-1, FH and FHR-5 were added. Binding of the three FH family proteins was detected with polyclonal anti-FH. Whilst the antibody shows less reactivity with FHR-5, due to the lower sequence identity to FH, than between FH and FHR-1, a stronger signal for FHR-5 was obtained compared with that for FHR-1 (**Fig. 3D**).

Confirmation of the mCRP binding site in FHR-1

To further confirm the C-terminal mCRP binding site in FHR-1, the mAb C18 was used, which binds in CCP20 of FH and CCP5 of FHR-1 (40, 41). This mAb strongly inhibited mCRP binding to FHR-1 (~70% inhibition under the experimental conditions), whereas a control mAb that binds in the middle portion of FH did not interfere with mCRP binding (**Fig. 4A**).

Because most FH autoantibodies that are associated with the autoimmune form of aHUS also bind within these FH domains and cross-react with FHR-1 (20, 40, 45), we tested three IgG preparations isolated from FH autoantibody positive aHUS patients. Of the three IgGs, two inhibited mCRP binding to FHR-1 (**Fig. 4B**), by ~70% and ~50%, respectively, while all three inhibited C3b binding (not shown).

Some of the aHUS-associated C-terminal FH mutations were shown to impair the binding of FH to CRP indicating the role of FH residues 1183, 1197, 1210 and 1215 in CRP binding (24). Because the same FHR-1 and FH domains were shown to include a binding site

for the CRP homolog pentraxin PTX3 (22, 23, 35), we analyzed the binding of PTX3 to 14 different recombinant FH CCPs 19-20 fragments containing single amino acid substitutions. This approach, similar to results obtained previously using peptide array (23), identified residues 1182-1186 and 1203-1215 relevant in PTX3 binding, thus at least partially overlapping with the mCRP binding site (**Fig. 4C**). In line with this, the two pentraxins mCRP and PTX3 partially competed for FHR-1 binding, mCRP caused a ~40% reduction in PTX3 binding at the tested highest concentration (**Fig. 4D**). The pentraxin binding sites, as well as the binding sites for C3b and sialic acid, are shown on a surface representation of the FH19-20 structure (**Fig. 4E**).

FHR-1 competes with FH for mCRP binding

Recent evidence supports a role for some of the FHR proteins as competitive inhibitors of FH on certain ligands, such as C3b, pentraxins and the extracellular matrix (10, 21, 35). Therefore, we investigated whether FHR-1 and FH compete for CRP binding due to the homologous mCRP binding sites in FHR-1 CCPs 4-5 and FH CCPs 19-20. To this end, the C-terminal FH fragment CCPs 15-20 was immobilized on microplate wells, and binding of mCRP to these domains in the presence of FHR-1 was measured. FHR-1 at 1 μ M concentration significantly inhibited mCRP binding to FH CCPs 15-20; FHR-1 caused a ~25% inhibition in binding as compared to the control protein HSA (**Fig. 5A**). FHR-1 did not compete with FHL-1 for mCRP (not shown).

To assess the functional effect of this competition, FHR-1 was added to normal human serum (**Fig. 5B**) and FH-depleted serum (**Fig. 5C**), and incubated on CRP-coated wells. Even when exogenous FHR-1 was added at 2 μ M concentration to 12.5% human serum, no significant increase in C3 deposition was detected. By contrast, FHR-5 at 300 nM significantly increased C3 deposition in both sera (**Fig. 5B and C**).

FHR-1 has no significant complement regulating activity for C3b and the terminal pathway

Because previous reports are controversial regarding FHR-1 as a complement inhibitor (12, 20, 21), we set out to clarify this issue. First the ability of FHR-1 to regulate the alternative pathway C3 convertase was measured. FHR-1 up to 1 μ M did not inhibit the binding of FB to C3b and the formation and activity of the C3bBb convertase (**Fig. 6A and 6B**). FHR-1 also did not interfere with the ability of FH to regulate the C3 convertase even if FHR-1 was added in 16-fold molar excess to FH, whereas FHR-5 at 10-fold molar excess to FH resulted in ~50% inhibition of FH decay accelerating activity (**Fig. 6C**).

The capacity of FHR-1 to inhibit the terminal pathway was assessed in serum. Activation of the alternative pathway was induced by addition of zymosan and the formation of soluble C5b-9 complexes was measured by ELISA. In this assay, 1 μ M (and even 2 μ M) FHR-1 did not inhibit zymosan-induced C5b-9 generation whereas addition of 1 μ M FH resulted in ~40% inhibition of C5b-9 formation (**Fig. 7**).

The FHR-1:mCRP interaction allows for enhanced C1q binding and classical pathway activation

To analyze if FHR-1 bound mCRP can still bind C1q, FHR-1 was immobilized in microplate wells and incubated with or without mCRP. Then serial dilutions of purified C1q were added and C1q binding was measured. C1q bound to FHR-1 in a dose-dependent manner and mCRP, particularly at lower C1q concentrations, significantly enhanced C1q binding (**Fig. 8A**). C1q showed background binding to gelatin, used as control, and mCRP did not affect this interaction. Similarly, mCRP bound to FHR-1 was able to bind the purified C1 complex (**Fig. 8B**).

We also assessed if this interaction supports classical pathway activation. FHR-1 was immobilized in microplate wells and preincubated or not with mCRP before incubating with 1% normal human serum. The bound mCRP on immobilized FHR-1 was able to activate the classical pathway and caused significantly enhanced C4 deposition (**Fig. 8C**). We also measured classical pathway activation on cell-derived ECM. ARPE-19 cells were cultured in 96-well plates and the ECM produced by these retinal pigmented epithelial cells was used in an ELISA setting. The washed, cell-free ECM was incubated with recombinant FHR-1 and mCRP as above, followed by addition of 1% human serum. On this ECM surface, mCRP when bound to FHR-1 significantly increased classical pathway activation measured as increased deposition of C4-fragments (**Fig. 8D**).

FHR-1 supports formation of the C3bBb convertase via C3b binding

FHRs lack the C3b and C3 convertase regulating activities of FH, but it was demonstrated that C3b binding to FHR-4 and FHR-5 can allow the formation of a fully active C3bBb convertase (35, 36). We therefore tested whether FHR-1 shares this ability. To this end, FHR-1 was immobilized on microplate wells and formation of C3bBb in vitro was measured by sequential incubation with C3b and FB plus FD plus properdin. A significant amount of C3bBb was formed on FHR-1 in this assay but this was significantly less than that formed on C3b (**Fig. 9A**). The less amount of C3bBb formed on FHR-1 in this particular assay is explained by the less C3b bound to FHR-1 compared to the amount of C3b bound to the plate surface when directly immobilizing C3b. The FHR-1 bound convertase was active as demonstrated by the conversion of C3 to C3a (**Fig. 9B**), suggesting that similar to FHR-4 and FHR-5, FHR-1 is able to support activation of the alternative pathway. FB and properdin did not directly bind to FHR-1 (**Supplemental Fig. 1**).

We also tested whether complement activation on FHR-1 occurs in serum. Wells coated with FHR-1, and as positive and negative controls, respectively, with FHR-4B and HSA, were incubated with normal human serum in buffer containing Mg^{2+} /EGTA to allow activation of only the alternative pathway. The binding of C3 fragments, FB and properdin to FHR-1 was detected, similar to FHR-4B, indicating the formation of the properdin-stabilized C3bBb alternative pathway convertase and complement activation in serum by FHR-1 (**Fig. 9C**).

To test if mCRP has an influence on this ability of FHR-1 to activate complement, *e.g.* due to partly overlapping binding site for C3b (see **Fig. 4E**), we first measured if mCRP-bound FHR-1 can still bind C3b. To this end, mCRP was immobilized in microplate wells and incubated with FHR-1, followed by the addition of C3b. This experiment showed that mCRP-bound FHR-1 was still able to bind C3b, but required higher C3b concentration than without mCRP (**Fig. 10A, Fig. S1**). In line with this, when ARPE-19 cell-derived ECM was used, mCRP on the ECM was able to bind FHR-1 and such bound FHR-1 could serve as a platform for the assembly of the C3bBb convertase (**Fig. 10B**).

Previously, FHR-1 was shown to bind to necrotic HUVEC (46). Therefore, HUVEC were necrotized by heat treatment, and the necrotic cells were incubated with FHR-1 alone or with mCRP followed by FHR-1, and exposed to 5% human serum. FHR-1 increased complement activation, as measured by the presence of FB as part of the alternative pathway convertase on the cell surface, which was enhanced by preincubation with mCRP (**Fig. 10C**). These data indicate that FHR-1 can enhance complement activation in cooperation with mCRP on certain non-cellular and cellular surfaces.

Discussion

Recent studies have changed our understanding of the functions of the FHR proteins (1), demonstrating a role of these proteins, including FHR-1, in enhancing complement activation, mainly via competition with the alternative pathway inhibitor FH. Although it is well established that FHR-1 does not compete with FH on host cell surfaces under normal healthy conditions (reviewed in (1)), very little is known about the FHR-1 ligands and the conditions under which competition between FHR-1 and FH may occur. Similarly, the possibility that FHR-1 has additional functions has not been sufficiently explored. CRP-complement cross-talk is implicated in the opsonophagocytic removal of dying cells and cellular debris (24, 47, 48). Because CRP-FH interaction was described to down-regulate inflammation (24, 31) and enhance the silent phagocytosis of apoptotic particles (24), and particularly impaired interaction between CRP and FH was suggested to be involved in the pathogenesis of AMD (32, 33), we investigated the ability of FHR-1 to bind CRP.

In this study we show that FHR-1, in its native form from serum and also in recombinant form, binds to CRP. As in the case of several of its ligand interactions, CRP binds to FHR-1 in a pH-dependent manner with increased binding at slightly acidic pH, a condition characteristic to inflammatory environments (**Fig. 2**). A more detailed analysis revealed that it is not the native, pentameric form of CRP which binds FHR-1 but the modified mCRP form, which is sometimes termed monomeric or denatured CRP, although this does not necessarily mean formation of CRP monomers or the requirement of harsh conditions. mCRP may be generated at acidic pH, increased temperature, in low- Ca^{2+} conditions or by binding to membranes and surfaces including plastic ones, *in vitro* (26, 27, 30, 42, 44, 49, 50). Remarkably, while CRP has been shown to bind FH also at lower pH (44), in our assays CRP binding to FHR-1 and FHR-5 could readily be detected under conditions when FH binding was not observed (**Fig. 2**).

The CRP binding site in FHR-1 is located in the C terminus of the protein (**Fig. 3 and 4**). This is not unexpected since CCPs 4-5 of FHR-1 are homologous with CCPs 19-20 of FH, which were previously shown to contain a major CRP binding site (24, 51). The FHR-1*A isoform is associated with AMD (52). We found no difference between the two FHR-1 isoforms in binding mCRP. The similar capacity of FHR-1*A and FHR-1*B to bind mCRP is likely explained by the fact that the CCPs 4-5 are identical in the two FHR-1 allelic variants.

FHR-1 indeed competed with the C-terminal FH fragment FH15-20 (**Fig. 5**), but not with FHL-1, which contains another mCRP binding site in CCP7. In serum, however, FHR-1 in contrast to FHR-5 caused only slightly but not significantly increased C3 deposition on CRP via competitive inhibition of FH (**Fig. 5**), likely due to its weaker binding to CRP compared with FH and FHR-5 (**Fig. 3D**). In addition, FH contains three CRP binding sites (24, 31, 51). For the FH:CRP interaction, an apparent K_D value of 4.2 μM was determined; for the FH fragment CCPs 6-8 (Y402 variant) a K_D value of 3.9 μM , and for CCPs 16-20 a K_D value of 15.3 μM (51). Thus, in FHR-1 the weaker CRP binding site of FH is conserved. Therefore, given the serum concentrations of FH and FHR-1 it is unlikely that under normal circumstances, even at enhanced CRP concentrations, functionally significant competition between the two FH-family proteins occurs that translates into enhanced complement activation. It cannot be excluded, however, that under certain conditions, such as local acidification, increase in FHR-1 concentration, or increased homo- and hetero-oligomerization between FHR-1 and FHR-5, complement deregulation may also take place on CRP. Such scenarios are feasible, because transcriptome analysis showed that the *CFHR1* gene is highly expressed in human retinal pigment epithelium (53), altered FHR-1 protein levels were described under inflammatory and disease conditions (54, 55), and mutation in *CFHR1* may result in higher order FHR-1 homo-oligomer formation with increased capacity

to out-compete FH (10). In addition, normal FH serum levels show significant variability in individuals, with reported ranges of 116-562 $\mu\text{g/ml}$ (56) and 124.4-402 $\mu\text{g/ml}$ (57).

The binding site in FHR-1 CCPs 4-5 of CRP apparently overlaps with that of the related pentraxin PTX3 (**Fig. 4**) (35). This binding site was confirmed using the mAb C18, which binds in FHR-1 CCP5 and inhibits both mCRP and PTX3 binding to FHR-1, and by analysis of recombinant mutant proteins; in addition, aHUS-associated FH autoantibodies may also impair these interactions (**Fig. 4**) (23, 24). In line with these results, we observed partial competition between mCRP and PTX3 for binding to FHR-1. During acute phase response, systemically strongly increased CRP levels may favour FHR-1 binding to CRP over PTX3, but when the amount of PTX3 is locally increased, PTX3 binding may prevail. Of note, PTX3 is expressed in human retinal pigment epithelial cells and is upregulated by IL-1 β and TNF- α (58).

Thus, it seems that, due to its weaker binding to CRP and PTX3 compared with FH, normally FHR-1 does not significantly deregulate complement activation via competition with FH on these ligands. Deregulation may, however, occur when avidity of FH to these ligands is decreased (e.g., due to FH mutations or FH polymorphisms), or if the avidity of FHR-1 is increased (e.g., due to mutation influencing the oligomeric state of the protein, or when high levels of ligand deposition enable divalent binding by FHR-1). It is possible that there is competition between FHR-1 and FH on other modified or newly exposed ligands, such as malondialdehyde epitopes and proteins of the extracellular matrix (currently under investigation). For example, FHR-1 could likely pass through the Bruch's membrane and may compete with FHL-1; even though FH has higher concentration than FHL-1, due to its size it cannot pass the pores in the fenestrated endothelium in the Bruch's membrane very efficiently (59). Under these conditions, interaction of FHR-1 with the extracellular matrix and CRP may enhance complement activation (**Fig. 8, Fig. 10**). The inverse association of the *CFHR1* gene deletion with AMD could partly be explained by our data: in AMD, local inflammation and pH change may favour FHR-1:CRP interaction, but the lack of FHR-1 would leave more room for the anti-inflammatory complement regulators FH and FHL-1.

Because of the debated complement inhibiting function of FHR-1, we examined its role in alternative pathway C3 convertase regulation and terminal pathway inhibition. In our assays, FHR-1 did not prevent assembly of the alternative pathway C3 convertase, did not accelerate the decay of the convertase, and did not competitively inhibit the convertase decay accelerating activity of FH (**Fig. 6**). Both FH and FHR-1 bind to C3b/C3d via their C termini and a recent study confirmed that in FHR-1 the C-terminal C3b binding site of FH is essentially conserved (60). Previously both weaker (a K_D value of 6.4 μM for the interaction of CCPs 1-3 of FHR-1 with C3b *versus* 2.6 μM for CCPs 18-20 of FH with C3b) (12, 61) and similarly strong (a K_D value of ~ 4 μM for the interaction of FHR-1-like mutant FH19-20 with C3b *versus* ~ 6 μM for FH19-20 (19, 62, 63) binding of FHR-1 to C3b as compared with FH were described; in our convertase assay no significant competition was observed. FHR-1 could also not inhibit soluble C5b-9 generation in our zymosan-induced complement activation assay (**Fig. 7**). Likewise, in a recent study we found no inhibition of serum C5b-9 generation caused by liposomes or cremophore EL micelles (64). Thus, our results and the majority of literature data (10, 21, 64) do not support the previously suggested terminal pathway inhibiting function of FHR-1.

Because C1q is one of the main complement ligands of CRP that can initiate classical pathway activation, we examined the influence of FHR-1 on this interaction. We found that FHR-1 bound mCRP could still bind C1q; the observed C1q binding to FHR-1 was significantly enhanced by mCRP (**Fig. 8**). C1q binding also occurred in the context of C1. Moreover, FHR-1-bound mCRP supported classical pathway activation, also on extracellular matrix produced *in vitro* by retinal pigmented epithelial cells (**Fig. 8**).

Importantly, FHR-1 by binding C3b allowed for the assembly of a functionally fully active alternative pathway C3 convertase and supported alternative pathway activation (**Fig. 9**). When FHR-1 was bound on mCRP, more C3b was required to form the C3bBb convertase on FHR-1 (**Fig. 10A and B**), likely due to the partially overlapping binding sites (**Fig. 4E**). This interaction, however, also supported alternative pathway activation on the surface of necrotic cells exposed to serum, indicating that mCRP and FHR-1 may cooperate in enhancing opsonization (**Fig. 10C**). Thus, we identify a new function of FHR-1 in the activation of complement, a role in striking contrast to that of the inhibitor FH, and similar to that described for FHR-4 and FHR-5 (35, 36).

In summary, CRP is identified and characterized as a novel ligand of FHR-1. Our results add to the growing body of evidence that, contrary to previous claim, FHR-1 is not an inhibitor of the terminal complement pathway. Instead, FHR-1 is shown to allow alternative pathway C3 convertase formation and alternative pathway activation. The FHR-1:mCRP interactions can enhance both classical and alternative pathway activation. Thus, FHR-1 promotes rather than inhibits complement activation.

References

1. Jozsi, M., A. Tortajada, B. Uzonyi, E. Goicoechea de Jorge, and S. Rodriguez de Cordoba. 2015. Factor H-related proteins determine complement-activating surfaces. *Trends Immunol* 36:374-384.
2. Skerka, C., Q. Chen, V. Fremeaux-Bacchi, and L. T. Roumenina. 2013. Complement factor H related proteins (CFHRs). *Mol Immunol* 56:170-180.
3. Krushkal, J., O. Bat, and I. Gigli. 2000. Evolutionary relationships among proteins encoded by the regulator of complement activation gene cluster. *Mol Biol Evol* 17:1718-1730.
4. Perez-Caballero, D., C. Gonzalez-Rubio, M. E. Gallardo, M. Vera, M. Lopez-Trascasa, S. Rodriguez de Cordoba, and P. Sanchez-Corral. 2001. Clustering of missense mutations in the C-terminal region of factor H in atypical hemolytic uremic syndrome. *Am J Hum Genet* 68:478-484.
5. Eyler, S. J., N. C. Meyer, Y. Zhang, X. Xiao, C. M. Nester, and R. J. Smith. 2013. A novel hybrid CFHR1/CFH gene causes atypical hemolytic uremic syndrome. *Pediatr Nephrol* 28:2221-2225.
6. Valoti, E., M. Alberti, A. Tortajada, J. Garcia-Fernandez, S. Gastoldi, L. Besso, E. Bresin, G. Remuzzi, S. Rodriguez de Cordoba, and M. Noris. 2015. A novel atypical hemolytic uremic syndrome-associated hybrid CFHR1/CFH gene encoding a fusion protein that antagonizes factor H-dependent complement regulation. *J Am Soc Nephrol* 26:209-219.
7. Venables, J. P., L. Strain, D. Routledge, D. Bourn, H. M. Powell, P. Warwicker, M. L. Diaz-Torres, A. Sampson, P. Mead, M. Webb, Y. Pirson, M. S. Jackson, A. Hughes, K. M. Wood, J. A. Goodship, and T. H. Goodship. 2006. Atypical haemolytic uraemic syndrome associated with a hybrid complement gene. *PLoS Med* 3:e431.
8. Dragon-Durey, M. A., C. Blanc, F. Marliot, C. Loirat, J. Blouin, C. Sautes-Fridman, W. H. Fridman, and V. Fremeaux-Bacchi. 2009. The high frequency of complement factor H related CFHR1 gene deletion is restricted to specific subgroups of patients with atypical haemolytic uraemic syndrome. *J Med Genet* 46:447-450.
9. Jozsi, M., C. Licht, S. Strobel, S. L. Zipfel, H. Richter, S. Heinen, P. F. Zipfel, and C. Skerka. 2008. Factor H autoantibodies in atypical hemolytic uremic syndrome correlate with CFHR1/CFHR3 deficiency. *Blood* 111:1512-1514.
10. Tortajada, A., H. Yebenes, C. Abarrategui-Garrido, J. Anter, J. M. Garcia-Fernandez, R. Martinez-Barricarte, M. Alba-Dominguez, T. H. Malik, R. Bedoya, R. Cabrera

- 597 Perez, M. Lopez Trascasa, M. C. Pickering, C. L. Harris, P. Sanchez-Corral, O.
598 Llorca, and S. Rodriguez de Cordoba. 2013. C3 glomerulopathy-associated CFHR1
599 mutation alters FHR oligomerization and complement regulation. *J Clin Invest*
600 123:2434-2446.
- 601 11. Timmann, C., M. Leippe, and R. D. Horstmann. 1991. Two major serum components
602 antigenically related to complement factor H are different glycosylation forms of a
603 single protein with no factor H-like complement regulatory functions. *J Immunol*
604 146:1265-1270.
- 605 12. Heinen, S., A. Hartmann, N. Lauer, U. Wiehl, H. M. Dahse, S. Schirmer, K. Gropp, T.
606 Enghardt, R. Wallich, S. Halbich, M. Mihlan, U. Schlotzer-Schrehardt, P. F. Zipfel,
607 and C. Skerka. 2009. Factor H-related protein 1 (CFHR-1) inhibits complement C5
608 convertase activity and terminal complex formation. *Blood* 114:2439-2447.
- 609 13. Skerka, C., R. D. Horstmann, and P. F. Zipfel. 1991. Molecular cloning of a human
610 serum protein structurally related to complement factor H. *J Biol Chem* 266:12015-
611 12020.
- 612 14. Abarrategui-Garrido, C., R. Martinez-Barricarte, M. Lopez-Trascasa, S. R. de
613 Cordoba, and P. Sanchez-Corral. 2009. Characterization of complement factor H-
614 related (CFHR) proteins in plasma reveals novel genetic variations of CFHR1
615 associated with atypical hemolytic uremic syndrome. *Blood* 114:4261-4271.
- 616 15. Blaum, B. S., J. P. Hannan, A. P. Herbert, D. Kavanagh, D. Uhrin, and T. Stehle.
617 2015. Structural basis for sialic acid-mediated self-recognition by complement factor
618 H. *Nat Chem Biol* 11:77-82.
- 619 16. Ferreira, V. P., A. P. Herbert, H. G. Hocking, P. N. Barlow, and M. K. Pangburn.
620 2006. Critical role of the C-terminal domains of factor H in regulating complement
621 activation at cell surfaces. *J Immunol* 177:6308-6316.
- 622 17. Jozsi, M., M. Oppermann, J. D. Lambris, and P. F. Zipfel. 2007. The C-terminus of
623 complement factor H is essential for host cell protection. *Mol Immunol* 44:2697-2706.
- 624 18. Kajander, T., M. J. Lehtinen, S. Hyvarinen, A. Bhattacharjee, E. Leung, D. E.
625 Isenman, S. Meri, A. Goldman, and T. S. Jokiranta. 2011. Dual interaction of factor H
626 with C3d and glycosaminoglycans in host-nonhost discrimination by complement.
627 *Proc Natl Acad Sci U S A* 108:2897-2902.
- 628 19. Morgan, H. P., C. Q. Schmidt, M. Guariento, B. S. Blaum, D. Gillespie, A. P. Herbert,
629 D. Kavanagh, H. D. Mertens, D. I. Svergun, C. M. Johansson, D. Uhrin, P. N. Barlow,
630 and J. P. Hannan. 2011. Structural basis for engagement by complement factor H of
631 C3b on a self surface. *Nat Struct Mol Biol* 18:463-470.
- 632 20. Strobel, S., C. Abarrategui-Garrido, E. Fariza-Requejo, H. Seeberger, P. Sanchez-
633 Corral, and M. Jozsi. 2011. Factor H-related protein 1 neutralizes anti-factor H
634 autoantibodies in autoimmune hemolytic uremic syndrome. *Kidney Int* 80:397-404.
- 635 21. Goicoechea de Jorge, E., J. J. Caesar, T. H. Malik, M. Patel, M. Colledge, S. Johnson,
636 S. Hakobyan, B. P. Morgan, C. L. Harris, M. C. Pickering, and S. M. Lea. 2013.
637 Dimerization of complement factor H-related proteins modulates complement
638 activation in vivo. *Proc Natl Acad Sci U S A* 110:4685-4690.
- 639 22. Deban, L., H. Jarva, M. J. Lehtinen, B. Bottazzi, A. Bastone, A. Doni, T. S. Jokiranta,
640 A. Mantovani, and S. Meri. 2008. Binding of the long pentraxin PTX3 to factor H:
641 interacting domains and function in the regulation of complement activation. *J*
642 *Immunol* 181:8433-8440.
- 643 23. Kopp, A., S. Strobel, A. Tortajada, S. Rodriguez de Cordoba, P. Sanchez-Corral, Z.
644 Prohaszka, M. Lopez-Trascasa, and M. Jozsi. 2012. Atypical hemolytic uremic
645 syndrome-associated variants and autoantibodies impair binding of factor h and factor
646 h-related protein 1 to pentraxin 3. *J Immunol* 189:1858-1867.

24. Mihlan, M., S. Stippa, M. Jozsi, and P. F. Zipfel. 2009. Monomeric CRP contributes to complement control in fluid phase and on cellular surfaces and increases phagocytosis by recruiting factor H. *Cell Death Differ* 16:1630-1640.
25. Black, S., I. Kushner, and D. Samols. 2004. C-reactive Protein. *J Biol Chem* 279:48487-48490.
26. Potempa, L. A., B. A. Maldonado, P. Laurent, E. S. Zemel, and H. Gewurz. 1983. Antigenic, electrophoretic and binding alterations of human C-reactive protein modified selectively in the absence of calcium. *Mol Immunol* 20:1165-1175.
27. Taylor, K. E., and C. W. van den Berg. 2007. Structural and functional comparison of native pentameric, denatured monomeric and biotinylated C-reactive protein. *Immunology* 120:404-411.
28. Pepys, M. B., and G. M. Hirschfield. 2003. C-reactive protein: a critical update. *J Clin Invest* 111:1805-1812.
29. Bottazzi, B., A. Doni, C. Garlanda, and A. Mantovani. 2010. An integrated view of humoral innate immunity: pentraxins as a paradigm. *Annu Rev Immunol* 28:157-183.
30. Biro, A., Z. Rovo, D. Papp, L. Cervenak, L. Varga, G. Fust, N. M. Thielens, G. J. Arlaud, and Z. Prohaszka. 2007. Studies on the interactions between C-reactive protein and complement proteins. *Immunology* 121:40-50.
31. Jarva, H., T. S. Jokiranta, J. Hellwage, P. F. Zipfel, and S. Meri. 1999. Regulation of complement activation by C-reactive protein: targeting the complement inhibitory activity of factor H by an interaction with short consensus repeat domains 7 and 8-11. *J Immunol* 163:3957-3962.
32. Laine, M., H. Jarva, S. Seitsonen, K. Haapasalo, M. J. Lehtinen, N. Lindeman, D. H. Anderson, P. T. Johnson, I. Jarvela, T. S. Jokiranta, G. S. Hageman, I. Immonen, and S. Meri. 2007. Y402H polymorphism of complement factor H affects binding affinity to C-reactive protein. *J Immunol* 178:3831-3836.
33. Skerka, C., N. Lauer, A. A. Weinberger, C. N. Keilhauer, J. Suhnel, R. Smith, U. Schlotzer-Schrehardt, L. Fritsche, S. Heinen, A. Hartmann, B. H. Weber, and P. F. Zipfel. 2007. Defective complement control of factor H (Y402H) and FHL-1 in age-related macular degeneration. *Mol Immunol* 44:3398-3406.
34. Hughes, A. E., N. Orr, H. Esfandiary, M. Diaz-Torres, T. Goodship, and U. Chakravarthy. 2006. A common CFH haplotype, with deletion of CFHR1 and CFHR3, is associated with lower risk of age-related macular degeneration. *Nat Genet* 38:1173-1177.
35. Csinci, A. I., A. Kopp, M. Zoldi, Z. Banlaki, B. Uzonyi, M. Hebecker, J. J. Caesar, M. C. Pickering, K. Daigo, T. Hamakubo, S. M. Lea, E. Goicoechea de Jorge, and M. Jozsi. 2015. Factor H-related protein 5 interacts with pentraxin 3 and the extracellular matrix and modulates complement activation. *J Immunol* 194:4963-4973.
36. Hebecker, M., and M. Jozsi. 2012. Factor H-related protein 4 activates complement by serving as a platform for the assembly of alternative pathway C3 convertase via its interaction with C3b protein. *J Biol Chem* 287:19528-19536.
37. Kuhn, S., and P. F. Zipfel. 1995. The baculovirus expression vector pBSV-8His directs secretion of histidine-tagged proteins. *Gene* 162:225-229.
38. Castiblanco-Valencia, M. M., T. R. Fraga, L. B. Silva, D. Monaris, P. A. Abreu, S. Strobel, M. Jozsi, L. Isaac, and A. S. Barbosa. 2012. Leptospiral immunoglobulin-like proteins interact with human complement regulators factor H, FHL-1, FHR-1, and C4BP. *J Infect Dis* 205:995-1004.
39. Hebecker, M., A. I. Okemefuna, S. J. Perkins, M. Mihlan, M. Huber-Lang, and M. Jozsi. 2010. Molecular basis of C-reactive protein binding and modulation of complement activation by factor H-related protein 4. *Mol Immunol* 47:1347-1355.

40. Bhattacharjee, A., S. Reuter, E. Trojnar, R. Kolodziejczyk, H. Seeberger, S. Hyvarinen, B. Uzonyi, A. Szilagyi, Z. Prohaszka, A. Goldman, M. Jozsi, and T. S. Jokiranta. 2015. The major autoantibody epitope on factor H in atypical hemolytic uremic syndrome is structurally different from its homologous site in factor H-related protein 1, supporting a novel model for induction of autoimmunity in this disease. *J Biol Chem* 290:9500-9510.
41. Oppermann, M., T. Manuelian, M. Jozsi, E. Brandt, T. S. Jokiranta, S. Heinen, S. Meri, C. Skerka, O. Gotze, and P. F. Zipfel. 2006. The C-terminus of complement regulator Factor H mediates target recognition: evidence for a compact conformation of the native protein. *Clin Exp Immunol* 144:342-352.
42. Mihlan, M., M. Hebecker, H. M. Dahse, S. Halbich, M. Huber-Lang, R. Dahse, P. F. Zipfel, and M. Jozsi. 2009. Human complement factor H-related protein 4 binds and recruits native pentameric C-reactive protein to necrotic cells. *Mol Immunol* 46:335-344.
43. Jokiranta, T. S., V. P. Jaakola, M. J. Lehtinen, M. Parepalo, S. Meri, and A. Goldman. 2006. Structure of complement factor H carboxyl-terminus reveals molecular basis of atypical haemolytic uremic syndrome. *Embo J* 25:1784-1794.
44. Hammond, D. J., Jr., S. K. Singh, J. A. Thompson, B. W. Beeler, A. E. Rusinol, M. K. Pangburn, L. A. Potempa, and A. Agrawal. 2010. Identification of acidic pH-dependent ligands of pentameric C-reactive protein. *J Biol Chem* 285:36235-36244.
45. Jozsi, M., S. Strobel, H. M. Dahse, W. S. Liu, P. F. Hoyer, M. Oppermann, C. Skerka, and P. F. Zipfel. 2007. Anti factor H autoantibodies block C-terminal recognition function of factor H in hemolytic uremic syndrome. *Blood* 110:1516-1518.
46. Chen, Q., M. Manzke, A. Hartmann, M. Buttner, K. Amann, D. Pauly, M. Wiesener, C. Skerka, and P. F. Zipfel. 2016. Complement Factor H-Related 5-Hybrid Proteins Anchor Properdin and Activate Complement at Self-Surfaces. *J Am Soc Nephrol* 27:1413-1425.
47. Gershov, D., S. Kim, N. Brot, and K. B. Elkon. 2000. C-Reactive protein binds to apoptotic cells, protects the cells from assembly of the terminal complement components, and sustains an antiinflammatory innate immune response: implications for systemic autoimmunity. *J Exp Med* 192:1353-1364.
48. Nauta, A. J., M. R. Daha, C. van Kooten, and A. Roos. 2003. Recognition and clearance of apoptotic cells: a role for complement and pentraxins. *Trends Immunol* 24:148-154.
49. Hakobyan, S., C. L. Harris, C. W. van den Berg, M. C. Fernandez-Alonso, E. G. de Jorge, S. R. de Cordoba, G. Rivas, P. Mangione, M. B. Pepys, and B. P. Morgan. 2008. Complement factor H binds to denatured rather than to native pentameric C-reactive protein. *J Biol Chem* 283:30451-30460.
50. Ji, S. R., Y. Wu, L. Zhu, L. A. Potempa, F. L. Sheng, W. Lu, and J. Zhao. 2007. Cell membranes and liposomes dissociate C-reactive protein (CRP) to form a new, biologically active structural intermediate: mCRP(m). *Faseb J* 21:284-294.
51. Okemefuna, A. I., R. Nan, A. Miller, J. Gor, and S. J. Perkins. 2010. Complement factor H binds at two independent sites to C-reactive protein in acute phase concentrations. *J Biol Chem* 285:1053-1065.
52. Martinez-Barricarte, R., S. Recalde, P. Fernandez-Robredo, I. Millan, L. Olavarrieta, A. Vinuela, J. Perez-Perez, A. Garcia-Layana, and S. Rodriguez de Cordoba. 2012. Relevance of complement factor H-related 1 (CFHR1) genotypes in age-related macular degeneration. *Invest Ophthalmol Vis Sci* 53:1087-1094.
53. Bennis, A., T. G. Gorgels, J. B. Ten Brink, P. J. van der Spek, K. Bossers, V. M. Heine, and A. A. Bergen. 2015. Comparison of Mouse and Human Retinal Pigment

- Epithelium Gene Expression Profiles: Potential Implications for Age-Related Macular Degeneration. *PLoS One* 10:e0141597.
54. Corbett, B. A., A. B. Kantor, H. Schulman, W. L. Walker, L. Lit, P. Ashwood, D. M. Rocke, and F. R. Sharp. 2007. A proteomic study of serum from children with autism showing differential expression of apolipoproteins and complement proteins. *Mol Psychiatry* 12:292-306.
 55. Narkio-Makela, M., J. Hellwage, O. Tahkokallio, and S. Meri. 2001. Complement-regulator factor H and related proteins in otitis media with effusion. *Clin Immunol* 100:118-126.
 56. Esparza-Gordillo, J., J. M. Soria, A. Buil, L. Almasy, J. Blangero, J. Fontcuberta, and S. Rodriguez de Cordoba. 2004. Genetic and environmental factors influencing the human factor H plasma levels. *Immunogenetics* 56:77-82.
 57. Hakobyan, S., A. Tortajada, C. L. Harris, S. R. de Cordoba, and B. P. Morgan. 2010. Variant-specific quantification of factor H in plasma identifies null alleles associated with atypical hemolytic uremic syndrome. *Kidney Int* 78:782-788.
 58. Woo, J. M., M. Y. Kwon, D. Y. Shin, Y. H. Kang, N. Hwang, and S. W. Chung. 2013. Human retinal pigment epithelial cells express the long pentraxin PTX3. *Mol Vis* 19:303-310.
 59. Clark, S. J., C. Q. Schmidt, A. M. White, S. Hakobyan, B. P. Morgan, and P. N. Bishop. 2014. Identification of factor H-like protein 1 as the predominant complement regulator in Bruch's membrane: implications for age-related macular degeneration. *J Immunol* 193:4962-4970.
 60. Hannan, J. P., J. Laskowski, J. M. Thurman, G. S. Hageman, and V. M. Holers. 2016. Mapping the Complement Factor H-Related Protein 1 (CFHR1):C3b/C3d Interactions. *PLoS One* 11:e0166200.
 61. Heinen, S., P. Sanchez-Corral, M. S. Jackson, L. Strain, J. A. Goodship, E. J. Kemp, C. Skerka, T. S. Jokiranta, K. Meyers, E. Wagner, P. Robitaille, J. Esparza-Gordillo, S. Rodriguez de Cordoba, P. F. Zipfel, and T. H. Goodship. 2006. De novo gene conversion in the RCA gene cluster (1q32) causes mutations in complement factor H associated with atypical hemolytic uremic syndrome. *Hum Mutat* 27:292-293.
 62. Ferreira, V. P., A. P. Herbert, C. Cortes, K. A. McKee, B. S. Blaum, S. T. Esswein, D. Uhrin, P. N. Barlow, M. K. Pangburn, and D. Kavanagh. 2009. The binding of factor H to a complex of physiological polyanions and C3b on cells is impaired in atypical hemolytic uremic syndrome. *J Immunol* 182:7009-7018.
 63. Herbert, A. P., D. Kavanagh, C. Johansson, H. P. Morgan, B. S. Blaum, J. P. Hannan, P. N. Barlow, and D. Uhrin. 2012. Structural and functional characterization of the product of disease-related factor H gene conversion. *Biochemistry* 51:1874-1884.
 64. Meszaros, T., A. I. Csinci, B. Uzonyi, M. Hebecker, T. G. Fulop, A. Erdei, J. Szebeni, and M. Jozsi. 2016. Factor H inhibits complement activation induced by liposomal and micellar drugs and the therapeutic antibody rituximab in vitro. *Nanomedicine* 12:1023-1031.

Footnotes:

This work was financially supported in part by the Hungarian Scientific Research Fund (OTKA, grant K 109055) and the Lendület Program of the Hungarian Academy of Sciences (grant LP2012-43 to M.J.). SRdeC is supported by the Spanish “Ministerio e Economía y Competitividad” (SAF2011-26583), the Autonomous Region of Madrid (S2010BMD-2316) and the European Union (Eurenomics). TSJ acknowledges research grants from the Sigrid Jusélius foundation and the Academy of Finland (grants 128646, 255922, and 259793).

¹Parts of this work were presented at the 15th European Meeting on Complement in Human Disease, June 27-30, 2015, Uppsala, Sweden (*Mol. Immunol.* 2015, 67:132-133).

²Corresponding author: Mihály Józsi, MTA-ELTE “Lendület” Complement Research Group, Department of Immunology, Eötvös Loránd University, Pázmány Péter sétány 1/c, H-1117 Budapest, Hungary; Phone: +36 1 3812175; Fax: +36 1 3812176; E-mail: mihaly.jozsi@gmx.net.

³Abbreviations used in this paper: aHUS, atypical hemolytic uremic syndrome; AMD, age-related macular degeneration; CCP, complement control protein domain; ECM, extracellular matrix; FHR, factor H-related; FHR-1, factor H-related protein 1; FHR-4, factor H-related protein 4; FHR-5, factor H-related protein 5; CRP, C-reactive protein; DPBS, Dulbecco’s phosphate-buffered saline; FB, factor B; FD, factor D; FH, factor H; FI, factor I; FP, factor P; HSA, human serum albumin; mCRP, modified monomeric form of CRP; NHS, normal human serum; pCRP, native pentameric form of CRP; PTX3, pentraxin 3.

Author contributions: M.J. initiated and supervised the study. Á.I.C., B.U. and M.J. designed the experiments. Á.I.C., Z.S., Z.B. and M.J. performed ligand binding and competition assays. Á.I.C., B.U., M.C. and É.K. performed convertase and complement activation assays. Á.I.C., B.U., M.C. and É.K. generated and produced recombinant proteins, A.T. and S.R. de C. isolated FHR-1 isoforms, Z.P. provided serum samples, T.S.J. provided recombinant mutant proteins, J.J.E.C. and S.M.L. generated and provided FHR fragments. All authors discussed the data, revised and approved the manuscript. Á.I.C. and M.J. wrote the manuscript with the help of the other authors.

Figure legends

Fig. 1. Schematic drawing of FH and the FHR-1 isoforms.

FH is built up of 20 CCP domains, of which CCPs 1-4 mediate complement regulatory activity and CCPs 7, and 19-20 mediate surface recognition by FH. The FHR-1 domains are shown aligned with the corresponding most related FH domains. The numbers above the domains indicate the percentage of amino acid sequence identity between the homologous domains. CCP3 of the FHR-1*B variant is identical with CCP18 of FH whereas CCP3 of FHR-1*A differs in three amino acid from CCP18 of FH. In addition, α and β glycoforms are differentiated based on glycosylation pattern (not shown).

Fig. 2. Binding of FHR-1 to CRP.

(A) Microplate wells were coated with gelatin and CRP, and after blocking, incubated with 50% normal human serum or PBS. Bound proteins were eluted with SDS-sample buffer, subjected to 10% SDS-PAGE and western blotting. The blot was developed using polyclonal anti-FH. Representative of three experiments.

(B) Microplate wells were coated with purified FH, recombinant FHR-1 and FHR-5 proteins, and HSA as negative control. Human serum with CRP level of 161 $\mu\text{g/ml}$ from a sepsis patient was added at different pH values. Bound CRP was detected with polyclonal anti-CRP. Data are means \pm SD derived from four independent experiments. $*p < 0.05$, $**p < 0.01$, one-way ANOVA.

(C) The experiment described in (B) was also performed using 5 $\mu\text{g/ml}$ (~ 43 nM) recombinant CRP. Data are means \pm SD derived from three independent experiments. $*p < 0.05$, $**p < 0.01$, one-way ANOVA.

Fig. 3. Comparison of the binding of pCRP and mCRP to the FHR proteins.

(A) Binding of the native pentameric CRP to recombinant FHR proteins and FH by ELISA. The FH family proteins and human serum albumin (HSA), used as negative control, were immobilized in equimolar concentrations (200 nM) in microplate wells, then incubated with recombinant CRP. CRP binding was determined using a polyclonal anti-CRP antibody. Data are means \pm SD derived from three independent experiments. $*p < 0.05$, $***p < 0.001$, two-way ANOVA.

(B) Binding of the monomeric form of CRP (mCRP), generated by urea/EDTA chelation, was investigated by ELISA. FHR proteins, FH and the homologous C-terminal two domains of all five FHR proteins were immobilized, and the binding of 10 $\mu\text{g/ml}$ mCRP was detected using a polyclonal anti-CRP antibody. Data are means \pm SD derived from three independent experiments. $***p < 0.001$, one-way ANOVA.

(C) Binding of increasing concentrations of mCRP to immobilized FHR-1*A and FHR-1*B isoforms was measured as in (B). No difference of mCRP binding to the two allelic isoforms of FHR-1 was detected by ELISA.

(D) Binding of increasing concentrations of FH, FHR-5 and FHR-1 to immobilized CRP was detected with polyclonal anti-FH antibody. HSA was used as control protein. Data are means \pm SEM derived from three independent experiments. The binding of each of FH, FHR-5 and FHR-1 was significantly different from that of HSA. $*p < 0.05$, $**p < 0.01$, and $***p < 0.001$, two-way ANOVA.

Fig. 4. Analysis of the mCRP binding site in FHR-1.

(A) To confirm the binding site in FHR-1, mCRP binding was measured in the presence of a monoclonal antibody (C18) which is known to bind to the C-terminal of FH and FHR-1. As a control antibody, A255 was used which binds to the middle region of FH. Data are means \pm SD derived from three independent experiments. $***p < 0.001$, one-way ANOVA.

(B) The binding of mCRP to immobilized FHR-1 was measured in the presence of IgG fractions isolated from healthy individuals (H1-H3) or from aHUS patients with FH autoantibodies (P1-P3). Data are normalized to mCRP binding in the absence of IgG and represent means \pm SD derived from three independent experiments. $***p < 0.001$, one-way ANOVA.

(C) To identify residues relevant in PTX3 binding, mutant FH 19-20 fragments were coated and after blocking and washing, 5 $\mu\text{g/ml}$ PTX3 was added to the wells. Bound PTX3 was measured using a polyclonal anti-PTX3 antibody. Data are means \pm SD derived from three independent experiments. $*p < 0.05$, $**p < 0.01$, and $***p < 0.001$, one-way ANOVA.

(D) Competition between mCRP and PTX3 for FHR-1. FHR-1 was coated and the binding of 5 $\mu\text{g/ml}$ PTX3 in the presence of mCRP was measured. Data are means \pm SD derived from three independent experiments. $*p < 0.05$, one-way ANOVA.

(E) The ligand binding sites (residues in black) were plotted on a FH19-20 surface representation (structure derived from Protein Data Bank, accession code 2G7I (43)) using PyMOL, based on the results shown in (C) for PTX3 and previous results for mCRP (24). The

main C3b and sialic acid interacting residues are indicated based on previous structural studies (15, 18, 19).

Fig. 5. FHR-1 competes with the C terminus of FH for mCRP binding.

(A) The C-terminal FH fragment FH 15-20 was immobilized in microplate wells, and binding of 5 µg/ml mCRP to these domains in the presence of 1 µM FHR-1 was measured using a polyclonal anti-CRP antibody. Data are means ± SD derived from three independent experiments. * $p < 0.05$, one-way ANOVA.

(B) CRP was immobilized and normal human serum was added in the absence or presence of recombinant FHR-1 protein (2 µM). The amount of deposited C3 fragments, due to CRP induced complement activation, was measured with a polyclonal anti-C3 antibody. Data are means ± SD derived from four independent experiments. *** $p < 0.001$, one-way ANOVA.

(C) The assay described above was also conducted using FH-depleted serum. Data are means ± SD derived from three independent experiments. ** $p < 0.01$, one-way ANOVA.

Fig. 6. FHR-1 has no significant complement regulatory activity at the level of the alternative pathway C3 convertase.

(A) The capacity of FHR-1 to inhibit the formation of the solid phase C3bBb alternative pathway C3 convertase was studied in this experiment. The convertase components FB, FD and properdin were added to coated C3b in the presence of FH (10 µg/ml), FHR-5 (10 µg/ml), FHR-1 (50 µg/ml) or BSA (50 µg/ml), and the amount of the assembled convertase was measured after incubation with a polyclonal anti-FB antibody. Data are means ± SD derived from three independent experiments. * $p < 0.05$, one-way ANOVA.

(B) After the assembly of the convertase as described above, purified human C3 was added and the amount of the generated C3a was detected with an ELISA Kit. Data are means ± SD derived from three independent experiments. *** $p < 0.001$, one-way ANOVA.

(C) To assess the effect of FHR-1 on the decay of the alternative pathway C3 convertase, pre-assembled C3 convertase was incubated with 2.5 µg/ml FH, 10 µg/ml FHR-1, 10 µg/ml FHR-5 or FH together with FHR-1 or FHR-5 of the same concentrations. The normalized data are means ± SD derived from three independent experiments. * $p < 0.05$, ** $p < 0.01$, one-way ANOVA.

Fig. 7. FHR-1 does not inhibit terminal pathway *in vitro*.

The alternative pathway was activated in NHS by adding 20 µg/ml zymosan and the capacity of FHR-1 to inhibit the terminal pathway was measured by detecting the formation of soluble C5b-9 complexes by ELISA. FHR-1 up to 2 µM did not inhibit zymosan induced C5b-9 generation. FH (1 µM) was used as control. Data are means ± SD derived from three independent experiments. * $p < 0.05$, one-way ANOVA.

Fig. 8. FHR-1 bound mCRP binds C1q and allows for classical pathway activation.

(A) FHR-1 was immobilized in microplate wells and incubated with or without 5 µg/ml mCRP. After washing, serial dilutions of purified C1q in the indicated concentrations were added and the C1q binding was measured with a polyclonal anti-C1q antibody. Gelatin was used as a negative control. Data are means ± SD derived from three independent experiments. The binding of C1q to FHR-1 was significantly different in the presence of mCRP compared with the binding in the absence of mCRP ($p < 0.0001$, two-way ANOVA).

(B) Binding of 10 µg/ml purified C1 complex to wells coated with 4 µg/ml recombinant FHR-1 and preincubated with 5 µg/ml mCRP as in (A) was measured using a polyclonal anti-C1q antibody. Wells coated with gelatin were used as a negative control. Data are means ± SD derived from three independent experiments. *** $p < 0.001$, one-way ANOVA.

(C) FHR-1 and gelatin were immobilized in microplate wells and preincubated or not with 5 $\mu\text{g/ml}$ mCRP. 1% normal human serum in DPBS containing $\text{Ca}^{2+}/\text{Mg}^{2+}$ (NHS) or NHS in DPBS containing 20 mM EDTA was added for 30 min at 37°C, then C4-fragment deposition was detected using a polyclonal anti-C4 antibody. Data represent means \pm SD from three independent experiments. $**p < 0.01$, one-way ANOVA.

(D) ARPE-19 cells were cultured in 96-well plates for 7 days. After removal of the cells, the cell-derived ECM was incubated sequentially with FHR-1 and mCRP, then exposed to 1% normal human serum (NHS) or NHS/EDTA for 30 min at 37°C. C4-fragment deposition was detected using a polyclonal anti-C4 antibody. Data are means \pm SD from three independent experiments. $**p < 0.01$, one-way ANOVA.

Fig. 9. FHR-1 supports rather than inhibits complement activation.

(A) Assembly of the C3bBb convertase on FHR-1. Recombinant FHR-1, BSA as negative control and C3b as positive control were immobilized in microplate wells, followed by incubation with 10 $\mu\text{g/ml}$ C3b. The alternative pathway C3 convertase was built up by adding purified FB, factor D and FP for 30 min at 37°C. The convertase was detected with polyclonal anti-FB antibody. Data are means \pm SD derived from four independent experiments. $**p < 0.01$, $***p < 0.001$, one-way ANOVA.

(B) Activity of the FHR-1-bound convertase was measured by adding 10 $\mu\text{g/ml}$ C3 to the wells for 1 h at 37°C. C3a generation was measured by Quidel's C3a ELISA kit. Data are means \pm SD derived from three independent experiments. $**p < 0.01$, one-way ANOVA.

(C) FHR-1 was immobilized on microplate wells and incubated with 10% normal human serum in 5 mM Mg^{2+} -EGTA buffer to allow only alternative pathway activation. Deposition of C3b, factor B (FB) and properdin (FP) was detected using the corresponding antibodies. FHR-4B was used as positive control and human serum albumin (HSA) was used as negative control. Data are means \pm SD derived from three independent experiments. $*p < 0.05$, $**p < 0.01$, $***p < 0.001$, one-way ANOVA.

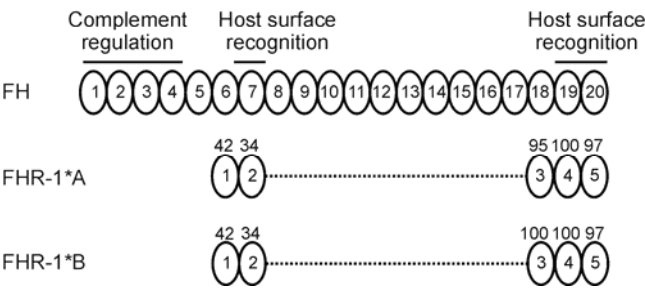
Fig. 10. FHR-1 activates the alternative pathway when bound to mCRP on surfaces.

(A) C3b can bind to mCRP-bound FHR-1. Microplate wells were coated with 5 $\mu\text{g/ml}$ mCRP, then incubated without or with 5 and 50 $\mu\text{g/ml}$ recombinant FHR-1. After washing, C3b was added in 20 $\mu\text{g/ml}$ (grey bars) or 50 $\mu\text{g/ml}$ (black bars) concentration. C3b binding was detected using a polyclonal anti-C3 antibody. Data are means \pm SD derived from three independent experiments. The binding of C3b was significantly enhanced in the presence of 50 $\mu\text{g/ml}$ FHR-1 compared with wells without FHR-1 ($*p < 0.05$, $**p < 0.01$, one-way ANOVA).

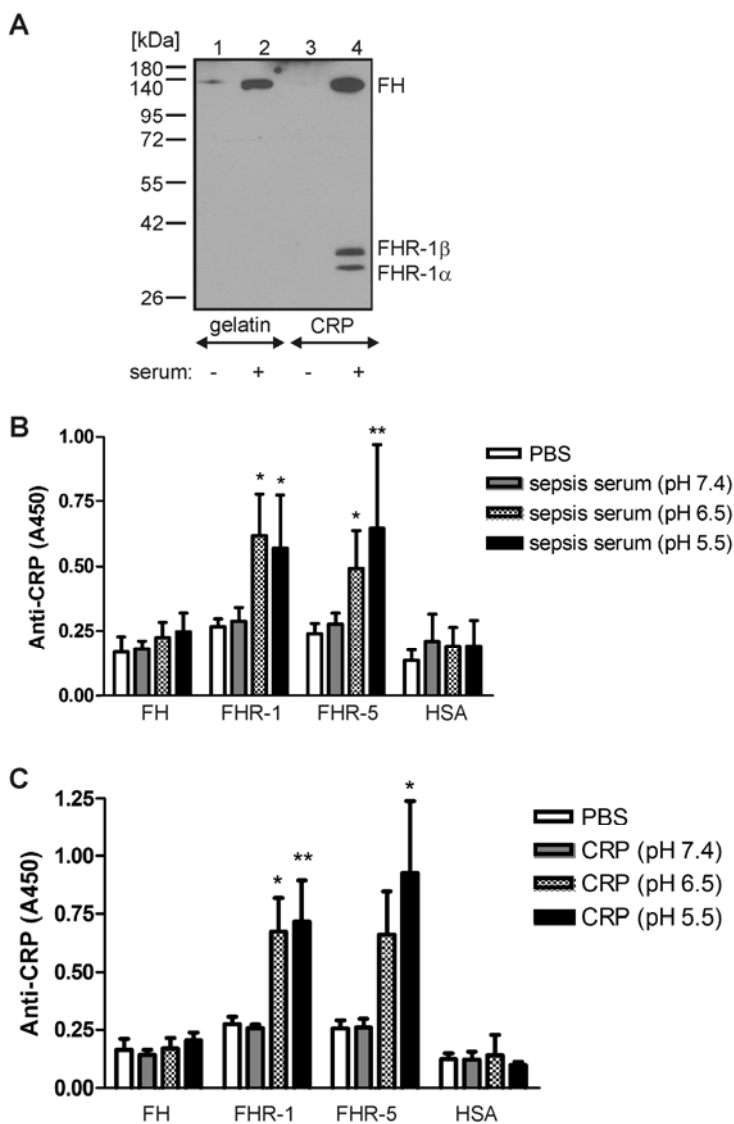
(B) Assembly of the alternative pathway C3 convertase C3bBb was measured on ECM produced by ARPE-19 cells *in vitro*, by incubating the washed, cell-free ECM with mCRP followed by FHR-1. After preincubating the ECM with 50 $\mu\text{g/ml}$ C3b, the convertase was built up by adding purified FB, FD and FP for 30 min at 37°C. The convertase was detected with anti-FB antibody. Data are means \pm SD derived from four independent experiments. $*p < 0.05$, one-way ANOVA.

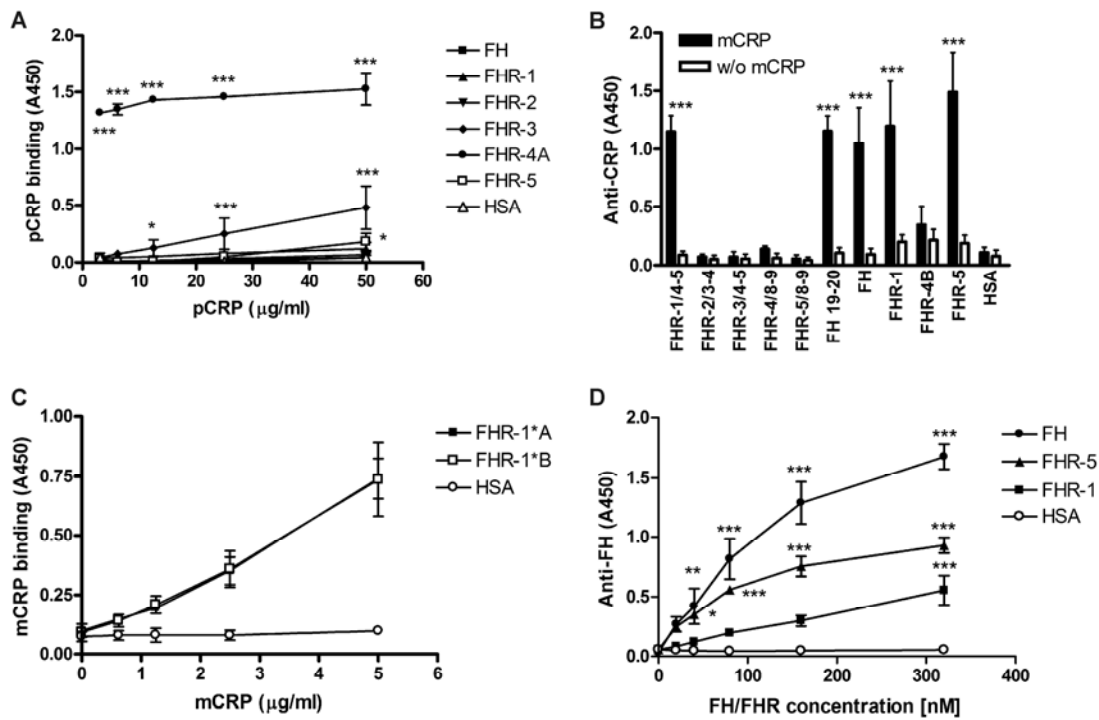
(C) Necrotic HUVEC were generated by heat treatment. The washed necrotic cells were preincubated or not with 2.5 $\mu\text{g/ml}$ mCRP, incubated with 25 $\mu\text{g/ml}$ FHR-1, then exposed to 5% normal human serum (NHS) for 30 min at 37°C. Activation of the alternative pathway was detected by flow cytometry using polyclonal anti-FB antibody and fluorescently labelled secondary antibody. Necrotic cells were identified by propidium iodide staining. Representative results out of three experiments are shown.

Csincsi et al. 2016
Figure 1

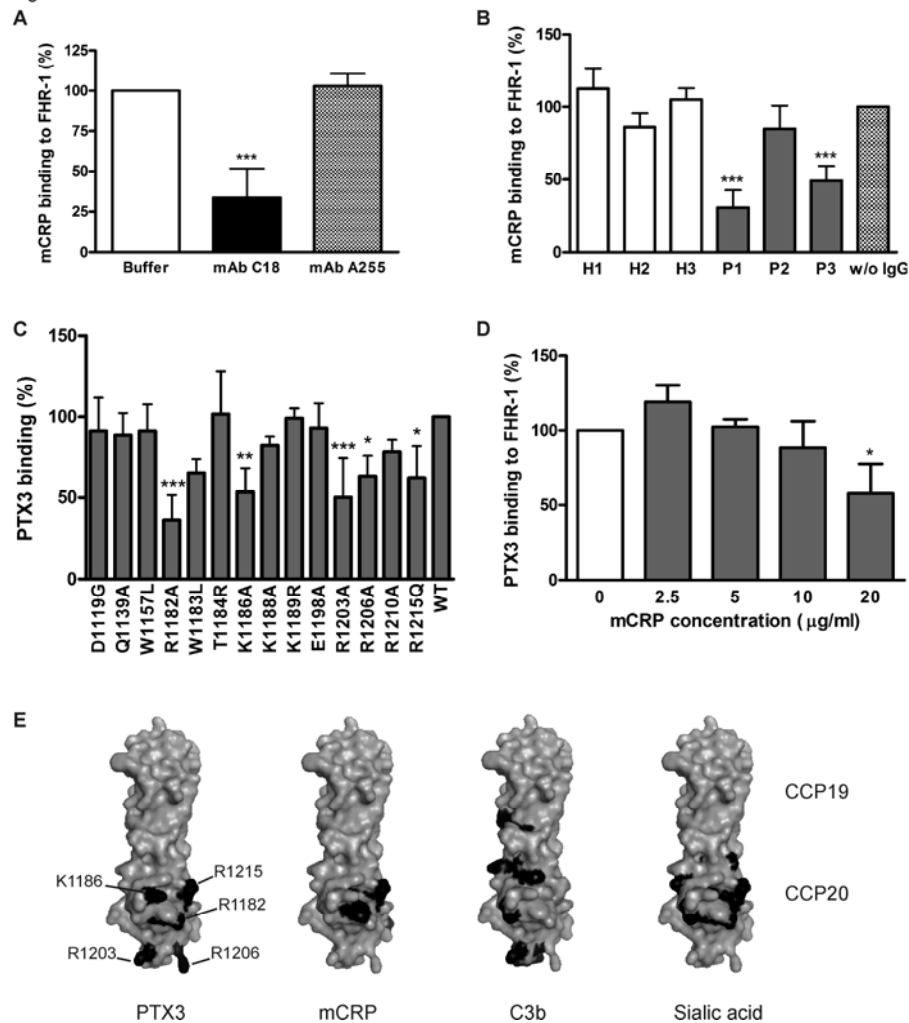


Csincsi et al. 2016
Figure 2

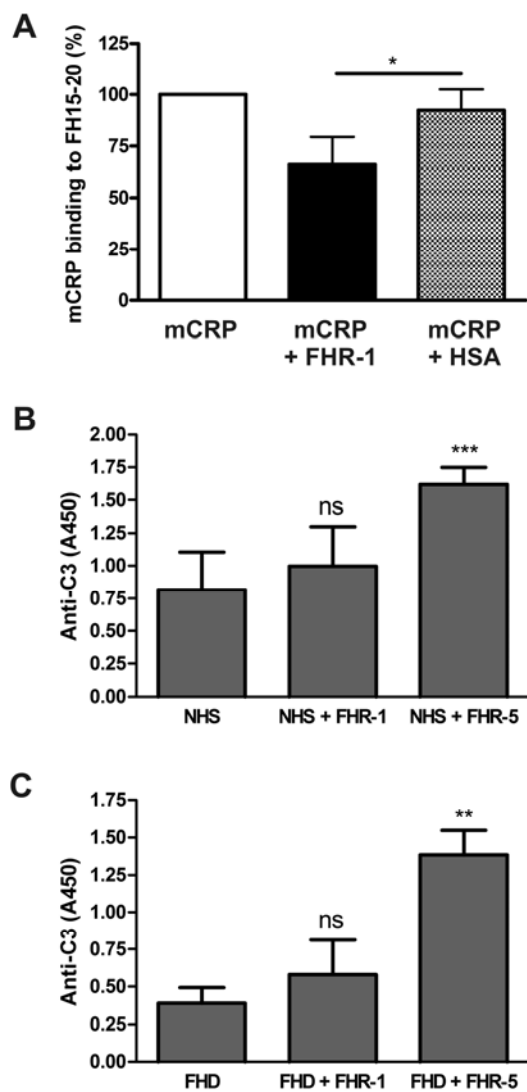




Csincsi et al. 2016
Figure 4

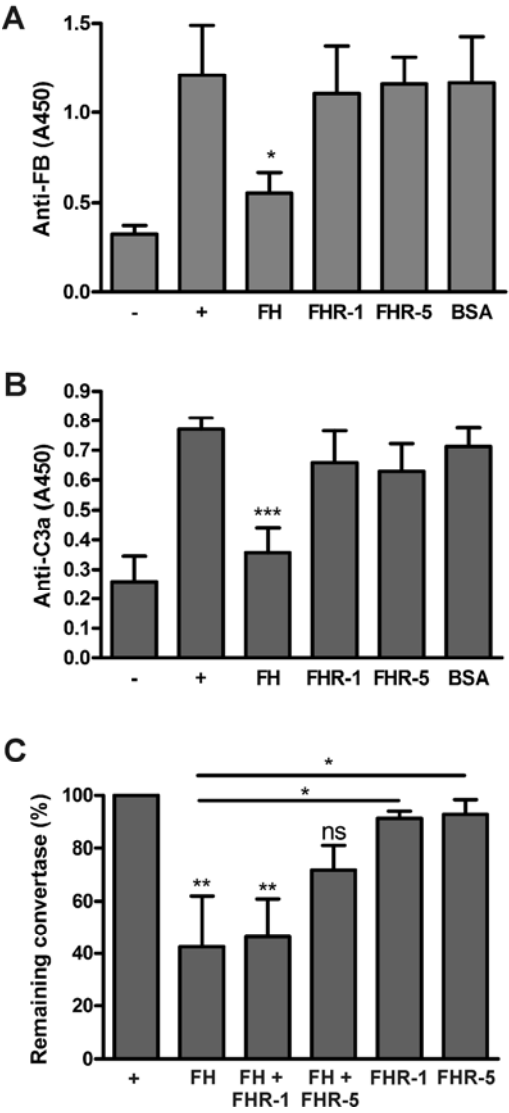


Csincsi et al. 2015
Figure 5

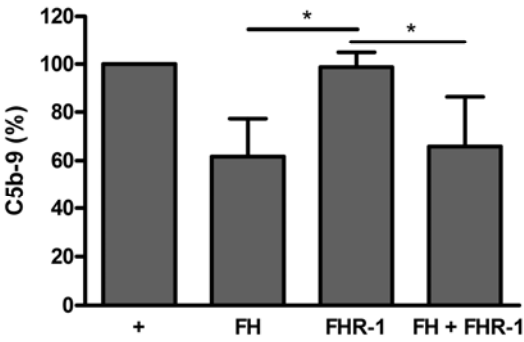


995
996

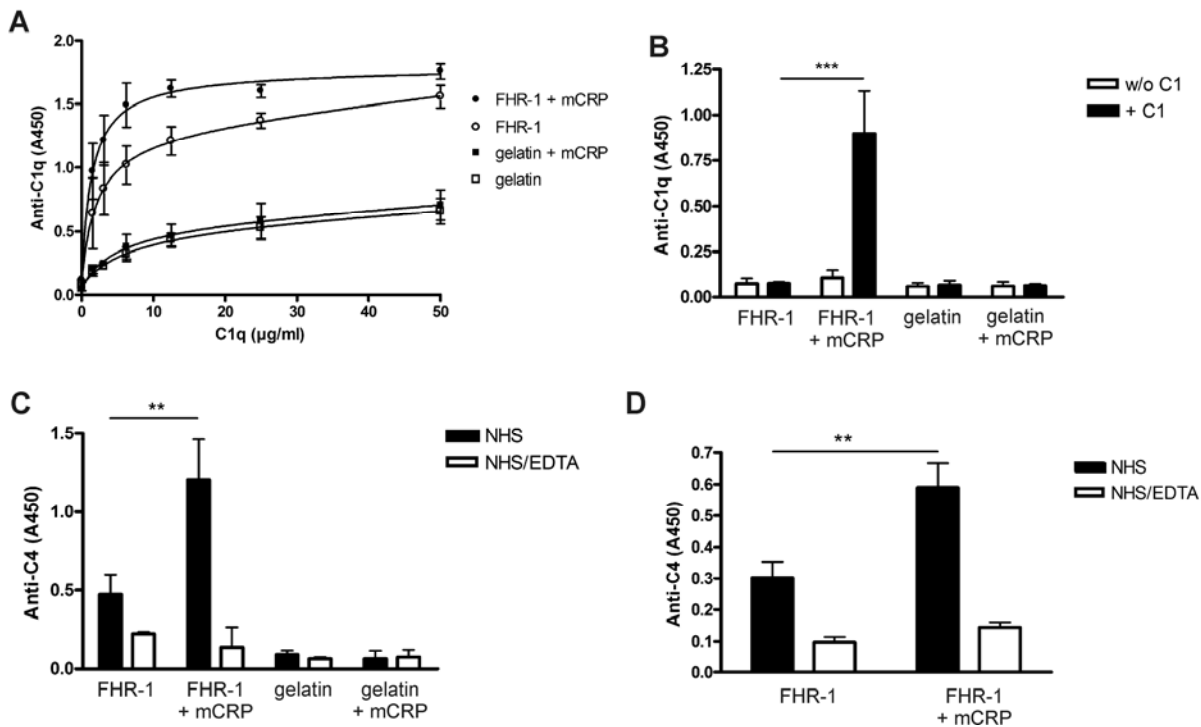
Csincsi et al. 2016
Figure 6



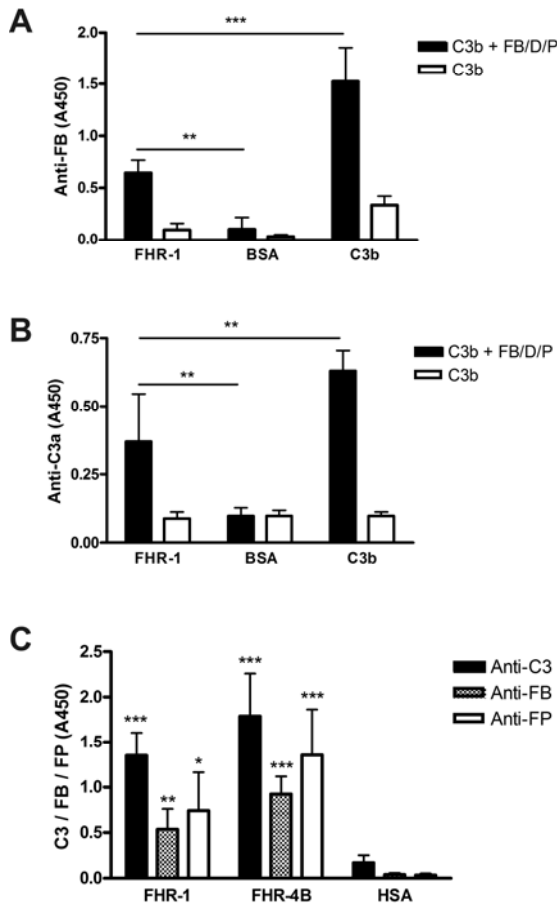
Csincsi et al. 2015
Figure 7



Csincsi et al. 2015
Figure 8

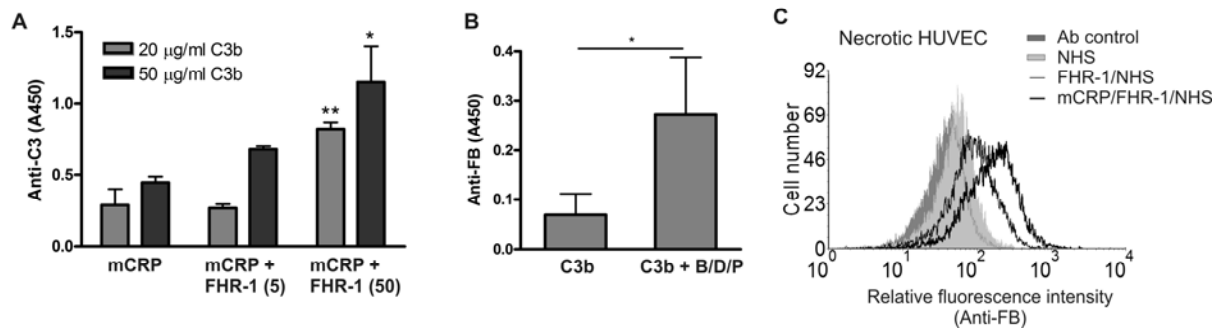


Csincsi et al. 2015
Figure 9



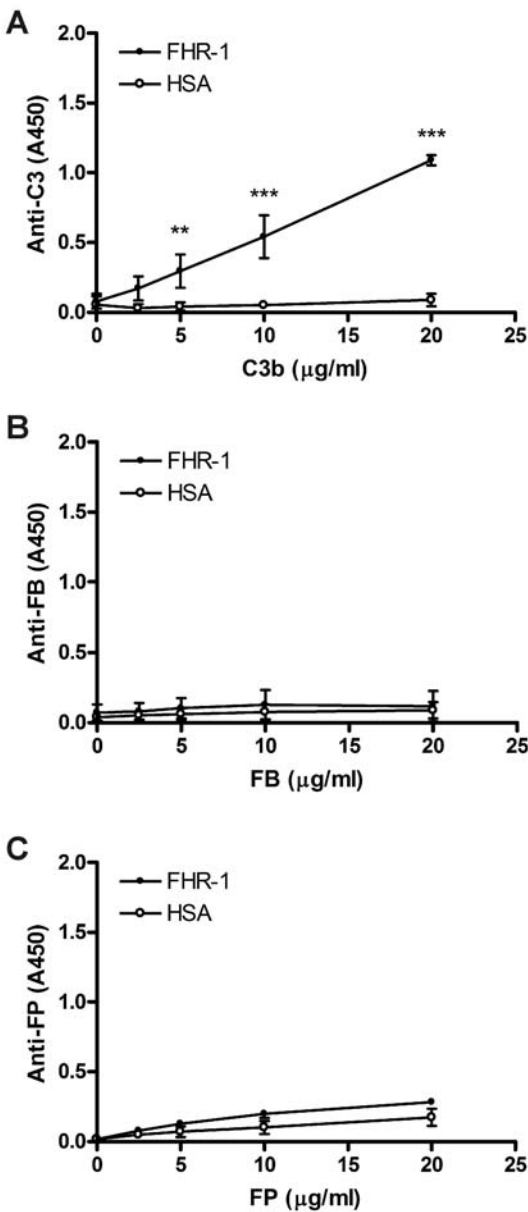
1006

Csincsi et al. 2017
Figure 10



1007
1008
1009

Fig. S1.



1010